Diamond & Related Materials 18 (2009) 501–504

Contents lists available at ScienceDirect

Diamond & Related Materials

journal homepage: www.elsevier.com/locate/diamond

Improved electrochemical performances by carbon nanocapsules as an electrocatalyst support for direct methanol fuel cells

Y.M. Chang, Y.C. Hsieh, P.W. Wu *

Department of Materials Science and Engineering, National Chiao Tung University, Hsinchu 30010, Taiwan

ARTICLE INFO

Available online 4 September 2008

Keywords:
Nanoparticles
Electrochemical properties
Catalytic processes
Direct methanol fuel cells

ABSTRACT

The carbon nanocapsules (CNCs) were evaluated as a catalyst support for direct methanol fuel cells (DMFC). The gas diffusion electrodes (GDE) of CNCs exhibited smaller pores, higher electrochemical surface areas, lower charge transfer resistances, and reduced resistivities as compared to those of Vulcan XC72R (VXC72R). The observed superiorities were attributed to their narrow size distributions and graphene layers on the perimeters. In addition, binary PtRu nanoparticles were synthesized and impregnated to the CNCs and VXC72R. The images from the transmission electron microscope indicated that the PtRu nanoparticles were dispersed better in the CNCs, resulting in relatively reduced particle sizes and greater uniformity. In cyclic voltammery, the PtRu/CNCs catalyzed GDEs revealed significantly larger current responses with lower onset potentials as compared to those of PtRu/VXC72R. Our results confirm the superb characteristic of CNCs as an electrocatalyst support for DMFC applications.

1. Introduction

Direct methanol fuel cells (DMFC) have received significant attention as the power source for portable electronics because their impressive specific energy (Wh g^{-1}) allows extended operation time [1,2]. The limiting factor for DMFC is the methanol oxidation at the anode. Hence, intensive activities have focused on the identification of effective electrocatalysts [3,4]. So far, binary alloys of PtRu [5] are the catalyst of choice for their facile conversion of methanol into carbon dioxide. Unfortunately, excess loading of PtRu is impractical since both the Pt and Ru are expensive noble metals. For better utilization of the catalyst mass, the PtRu particles are dispersed in a carbonaceous substrate. This is a common practice in gas diffusion electrodes (GDE) where the nanoparticulate electrocatalysts are evenly distributed onto a conductive matrix with high surface area, resulting in a large mass activity (mA mg^{-1}). In particular, substantial improvements in the catalytic performances were observed from the carbon supported catalysts as compared to the unsupported ones [6]. To date, a variety of carbonaceous materials have been explored as catalyst supports. They include typical carbon blacks like Vulcan XC72R (VXC72R), Black Pearls, and Shawiningan Black, as well as carbons in less familiar forms such as carbon nanotubes and carbon spherules [7–12]. The requirements for a desirable catalyst support are reasonably high surface area, superb corrosion resistance, and optimized pore size, attributes that can be found in the VXC72R.

Earlier studies of GDEs for alkaline fuel cells (AFC) indicated notable catalytic enhancements from catalysts supported on the carbon nanocapsules (CNCs) [13,14]. The CNCs are composed of near-spherical particles with great uniformity in sizes. Their impressive behaviors in alkaline electrolyte are rather encouraging. Unfortunately, the concern of electrolyte poisoning by ambient CO_2 limits AFC's practical opportunities [15]. In contrast, system using acidic electrolyte such as DMFC is more suitable to commercial applications. Hence, it would be of considerable interest to study the CNCs in DMFC. In this research, we carried out materials characterizations and electrochemical analysis on the GDEs from CNCs and PtRu/CNCs. Identical processes were repeated on the VXC72R serving as the reference.

2. Experimental section

2.1. Materials synthesis

The CNCs were prepared by a flame combustion method in which mixtures of C_2H_2 and O_2 underwent an incomplete combustion to form nanoparticulate carbon powders. Detailed synthetic parameters for the CNCs formation have been reported by Liu and Li [16]. Commercially available VXC72R (Cabot Inc.) was also used as catalyst support. In following electrochemical characterizations, nanoparticles of PtRu were employed as the catalyst supported on the CNCs and VXC72R for methanol oxidation in acidic electrolyte. The fabrication of PtRu was conducted by a chemical reduction route. First, 2.00 g of carbon powders (CNCs or VXC72R) were dispersed in 20 mL of solvent containing deionized water and ethanol (1:1 in vol. ratio) for 2 h at room temperature. The other solution was formulated by dissolving 0.25 g of $H_2PtCl_6{\cdot}6H_2O$ (99.90 wt.%), 0.10 g of $RuCl_3$ (99.98 wt.%), and 0.09 g of citric acid (1:1:2 in mol. ratio) in 20 mL of deionized water for 2 h at room temperature. Subsequently, both solutions were mixed

* Corresponding author. Tel.: +886 35131227; fax: +886 35724727.
E-mail address: ppwu@mail.nctu.edu.tw (P.W. Wu).

0925-9635/$ – see front matter © 2008 Elsevier B.V. All rights reserved.
doi:10.1016/j.diamond.2008.08.003

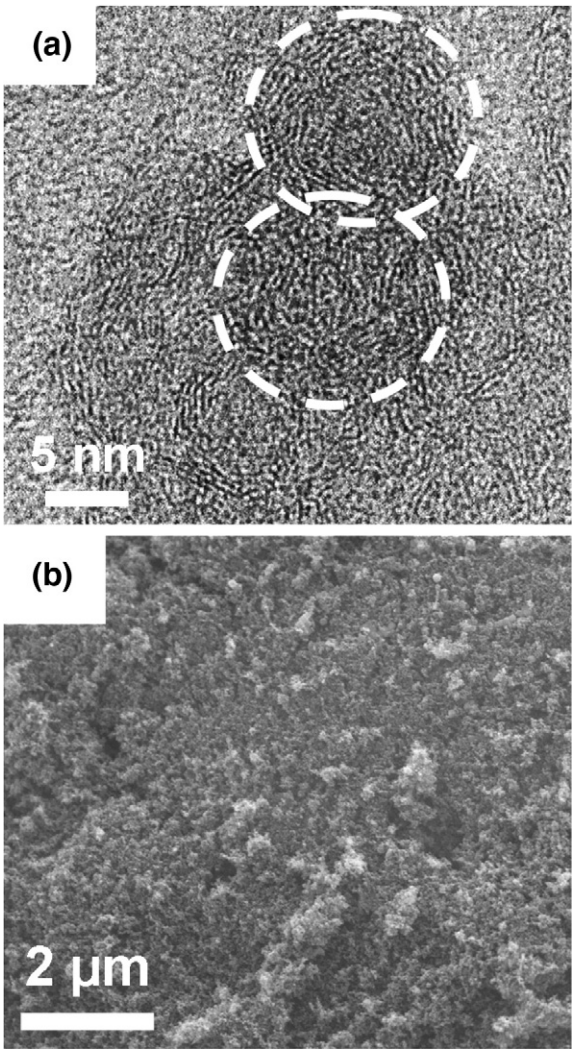

Fig. 1. The images of CNCs from (a) HRTEM and (b) SEM.

along with 0.73 g of $NaBH_4$ as the reducing agent. Afterwards the mixture was kept at 60 °C for 6 h, allowing complete reduction of Pt and Ru cations. Lastly, the suspension was filtered and washed followed by air drying at 90 °C for 24 h. The resulting PtRu supported carbon powders contain 20 wt.% PtRu.

2.2. Materials characterizations

High-resolution transmission electron microscope (HRTEM, Philips Tecnai-20) and scanning electron microscope (SEM, Jeol JSM-6700) were used to characterize the morphologies of CNCs, as well as the PtRu supported on the CNCs and VXC72R. The values for their surface area were determined by a BET (Micromeritics Tristar 3000). Phase confirmation of the PtRu nanoparticles was carried out by X-ray diffraction (XRD, Siemens D5000) from 10 to 80° with Cu K_α of 0.154 nm. We also adopted measurements in the contact angle (Kruss GH-100) and pore size (PMI Capillary Flow Porometer) to evaluate the hydrophobicity and pore size distributions of the GDEs from CNCs and VXC72R. In addition, the resistivity of the GDEs was recorded by a four-point-probe (AIT CMT-SR1000N).

2.3. Electrochemical analysis

GDEs from the CNCs and VXC72R, as well as GDEs from the PtRu/CNCs and PtRu/VXC72R were selected for electrochemical evaluations. A noncatalyzed GDE was used as the starting substrate. It was fabricated by preparing a dispersion including 70 wt.% Shawinigan Acetylene Black (Chevron) and 30 wt.% poly(tetrafluorethylene) (PTFE) followed by depositing onto a carbon cloth (E-TEK) and a heat treatment at 350 °C for 30 min in air. The resulting weight of the noncatalyzed GDE is 22 mg cm^{-2}. For preparation of the catalyzed GDEs, 8.00 mg of PtRu/CNCs (or PtRu/VXC72R), 2.50 mg of Nafion solution (5 wt.%), and 5 mL of deionized water were mixed to form an ink dispersion. The ink dispersion was deposited repeatedly onto the noncatalyzed GDE (2×2 cm^2) followed by a heat treatment at 100 °C for 30 min to remove residual solvents. The net catalyst loading for the PtRu/CNCs (or PtRu/VXC72R) was kept at 2 mg cm^{-2}. Similar procedures were performed on the noncatalyzed GDEs to fabricate GDEs of CNCs and VXC72R.

Electrochemical measurements such as cyclic voltamemetry (CV) and impedance analysis were carried out in a three-electrode arrangement using EG&G 263A and 1025. The Pt foil and Ag/AgCl were used as the counter and reference electrodes, respectively. The CVs for the GDEs of CNCs and VXC72R were conducted in 0.5 M H_2SO_4 electrolyte at a scan rate of 20 mV s^{-1} for a potential range of 0–0.7 V. The results from impedance analysis were obtained at −0.4 V (vs. open circuit voltage) with a 10 mV stimulus for frequency between 0.001–100 k Hz in electrolyte of 1 M H_2SO_4. The CVs for catalyzed GDEs were recorded in electrolyte of 1 M H_2SO_4 and 1 M CH_3OH for a potential range of −0.2–0.9 V at a scan rate of 20 mV s^{-1}. All the electrochemical characterizations were conducted at room temperature with a working electrode surface of 0.79 cm^2.

3. Results and discussion

3.1. Properties of the as-prepared CNCs powders

Fig. 1 provides images of the CNCs from HRTEM and SEM. As shown in Fig. 1(a), the CNCs appeared near-spherical in shape with a diameter of 10–15 nm. In addition, the image suggested a core-shell structure with graphene layers on the perimeters encompassing a hollow core. Fig. 1(b) presents the SEM picture revealing foam-like aggregates, indicating reasonable uniformity in sizes. Conventional wisdom in the GDE fabrications has established that size uniformity is beneficial for dense packing while graphene layers infer enhanced conductivity. Therefore, the CNCs are likely to be a promising candidate for catalyst support. In addition, the surface area of CNCs was measured at 333 m^2 g^{-1}, a value that is considered suitable for electrode applications. In contrast, the surface area of VXC72R was 254 m^2 g^{-1}.

A delicate balance between the gas transport and water removal is required for proper GDE operations. Hence, it is necessary to evaluate their hydrophobic characteristics. The GDEs from CNCs and VXC72R

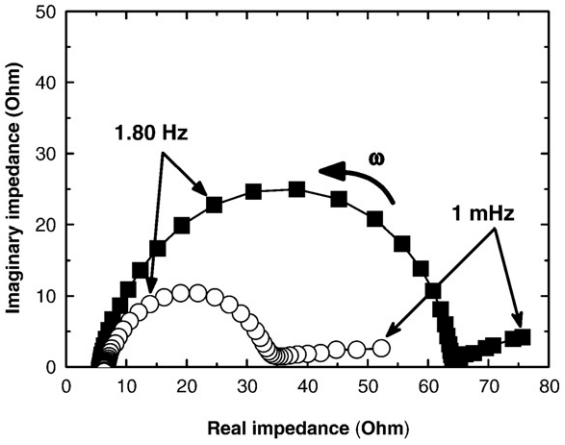

Fig. 2. The impedance spectra of GDEs from the CNCs (○) and VXC72R (■).

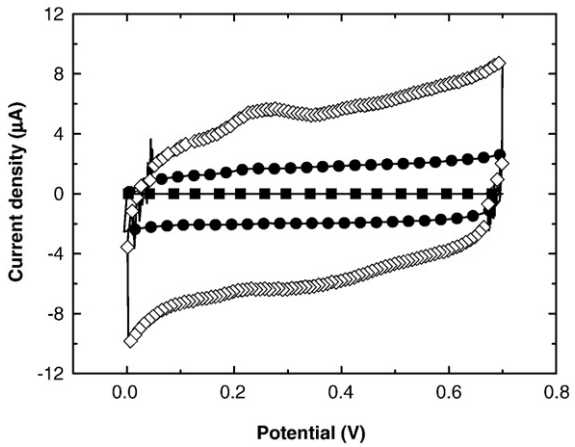

Fig. 3. The CV curves from the noncatalyzed GDE (■), as well as GDEs of CNCs (◊) and VXC72R (●).

exhibited contact angles of 105.84 and 104.51°, suggesting similar surface natures. The resistivities of the GDEs from CNCs and VXC72R were also measured at 46.52 and 54.73 mΩ-cm, respectively. These results agree with earlier TEM observations that confirm better electrical conductivity from the CNCs. In addition, the pores with the largest volume percentage from the GDEs of CNCs and VXC72R were 85.56 and 93.20 nm, respectively. This indicates that uniform and relatively smaller CNCs were able to form reduced pores in the GDE structure.

Fig. 2 demonstrates the Nyquist plot from the GDEs of CNCs and VXC72R. The spectra showed semicircles at high frequencies and linear tails at low frequencies. In impedance analysis, the appearance of semicircle is attributed to the coupled process of charge transfer resistance (R_{ct} in Ω-cm^2) and double-layer capacitance (C_{dl} in F cm^{-2}) on the GDE surface [17]. Hence, the value of R_{ct} can be deduced from the diameter of the semicircle. In addition, the intercept at the *x*-axis in the high frequency domain indicates the resistivity of the electrolyte. Accordingly, we determined the R_{ct} to be 19.79 and 41.57 Ω-cm^2 from GDEs of CNCs and VXC72R, respectively. The reduced R_{ct} value from the CNCs is likely resulted from their higher electrical conductivity.

3.2. Electrochemical evaluations of the CNCs derived GDEs

Fig. 3 exhibits the CV curves for the noncatalyzed GDE, as well as the GDEs of CNCs and VXC72R in electrolyte of 0.5 M H_2SO_4. Generally, the current responses from the voltage sweepings represent absorption and desorption of ions [18]. Hence, the area encircled reflects the area available for capacitive charges. Apparently, the noncatalyzed GDE revealed a negligible capacity of 4.58×10^{-8} C. Likewise, the GDE with VXC72R was able to accumulate a moderate 4.15×10^{-5} C. In contrast, the GDE with CNCs demonstrated a much larger total charge of 1.26×10^{-4} C. This value amounts to 304% enhancement from that of VXC72R. The CV scans confirm the GDE of CNCs with a substantially increased electrochemical active area.

HRTEM images of the PtRu supported on the CNCs and VXC72R are provided in Fig. 4. In our chemical synthesis, particles of PtRu were formed with sizes in 2–8 nm. As clearly shown, the CNCs seem to disperse the PtRu in better way; relatively smaller particle size and greater uniformity in distribution. In contrast, the PtRu supported on the VXC72R exhibited notable aggregation behaviors, which is undesirable from catalyst utilization standpoint. Although many possibilities exist for the observed phenomenon, the exact nature of the dispersing advantage from CNCs is unclear at this moment.

Fig. 5 presents the XRD patterns of PtRu supported on the CNCs and VXC72R. Apparently, the PtRu on both samples demonstrated a fcc phase, inferring complete alloying of Pt and Ru. Due to the size of the

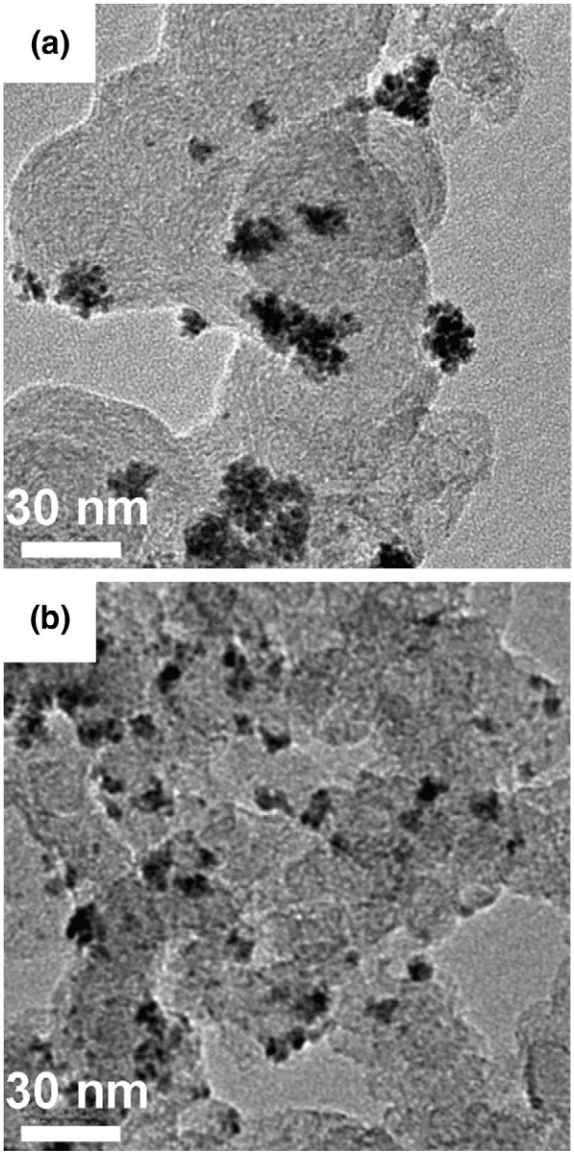

Fig. 4. The HRTEM images of PtRu nanoparticles supported on the (a) VXC72R and (b) CNCs.

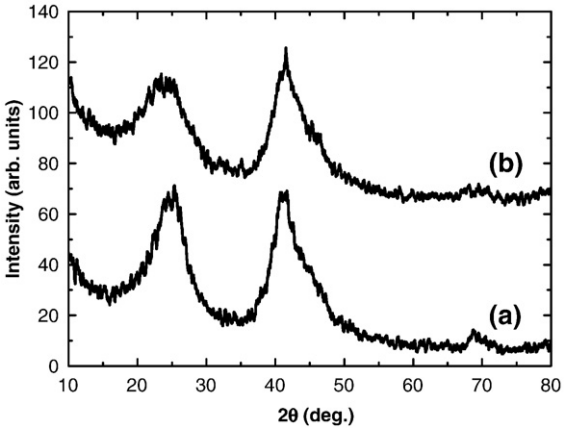

Fig. 5. The XRD patterns of PtRu nanoparticles supported on the (a) VXC72R and (b) CNCs.

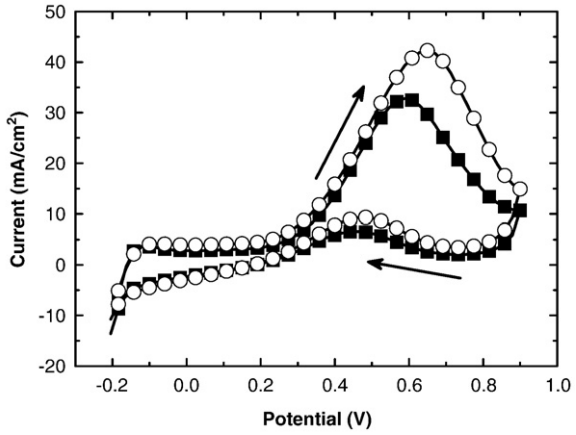

Fig. 6. The CV curves from the GDEs catalyzed by PtRu/VXC72R (■) and PtRu/CNCs (○).

PtRu particles, it is expected to observe those broad diffraction peaks. Combining the HRTEM images in Fig. 4 and XRD patterns of Fig. 5, we positively conclude that the nanoparticles of PtRu were successfully synthesized and dispersed in the CNCs and VXC72R.

The CV scans of GDEs catalyzed by the PtRu supported on the CNCs and VXC72R are demonstrated in Fig. 6. Comprehensive review on PtRu for fuel cell applications was provided recently by Petrii [19]. The areas underneath the CV curves indicate the amount of methanol undergoing the oxidation reaction [20]. Evidently, there appeared strong anodic current responses and weak cathodic ones. These patterns are consistent with what were reported previously by Tsai et al. [21,22]. The onset potentials for the PtRu supported on the CNCs and VXC72R were determined at 0.212 and 0.233 V, respectively. We would like to emphasize that the anodic peak current and the area in the CV scan were much larger for the PtRu supported on the CNCs. We surmise that smaller PtRu particles and better distribution occurring on the CNCs enable the observed improvements in catalysis. This behaviour agrees with our earlier results confirming the superiority of CNCs over VXC72R as a catalyst support for DMFC.

4. Conclusions

The CNCs were evaluated as a catalyst support in acidic electrolyte for DMFC. Owing to their narrow size distributions and graphene layers on the perimeters, the CNCs derived GDEs demonstrated smaller pores, higher electrochemical surface areas, lower R_{ct} values, and reduced resistivities as compared to those of VXC72R. In addition, the PtRu nanoparticles were found to disperse better in the CNCs, as evident from relatively reduced particle sizes and better uniformity. In comparison with PtRu/VXC72R, the PtRu/CNCs presented significantly larger CV responses with lower onset potentials. Our results indicate the CNCs to be an excellent catalyst support for DMFC applications.

Acknowledgments

The authors thank the National Science Council of Taiwan for financial grant (NSC-96-2221-E-009-110). Carbon nanocapsules were kindly provided by Professor Yuan-Yao Li of National Chung Cheng University.

References

[1] M. Winter, R.J. Brodd, Chem. Rev. 104 (2004) 4245.
[2] H. Liu, C. Song, L. Zhang, J. Zhang, H. Wang, D.P. Wilkinson, J. Power Sources 155 (2006) 95.
[3] J.H. Choi, K.W. Park, B.K. Kwon, Y.E. Sung, J. Electrochem. Soc. 150 (2003) A973.
[4] K.W. Park, J.H. Choi, S.A. Lee, C. Pak, H. Chang, Y.E. Sung, J. Catalysis 224 (2004) 236.
[5] T.R. Ralph, M.P. Hogarth, Platinum Metals Rev. 46 (2002) 117.
[6] Y.M. Chang, P.W. Wu, C.Y. Wu, Y.F. Hsieh, J.Y. Chen, Electrochem. Solid-State Lett. 11 (2008) B47.
[7] K. Han, J. Lee, H. Kim, Electrochim. Acta 52 (2006) 1697.
[8] G. Wang, G. Sun, Z. Zhou, J. Liu, Q. Wang, S. Wang, J. Guo, S. Yang, Q. Xin, B. Yi, Electrochem. Solid-State Lett. 8 (2005) A12.
[9] M. Maja, C. Orecchia, M. Strano, P. Tosco, M. Vanni, Electrochim. Acta 46 (2000) 423.
[10] C.C. Chen, C.F. Chen, C.H. Hsu, I.H. Li, Diamond Relat. Mater. 14 (2005) 770.
[11] R. Yang, X. Qiu, H. Zhang, J. Li, W. Zhu, Z. Wang, X. Huang, L. Chen, Carbon 43 (2005) 11.
[12] A.L. Dicks, J. Power Sources 156 (2006) 128.
[13] C.Y. Wu, P.W. Wu, P. Lin, Y.Y. Li, Y.M. Lin, J. Electrochem. Soc. 154 (2007) B1059.
[14] Y.M. Lin, Y.M. Chang, P.W. Wu, P. Lin, Y.Y. Li, C.Y. Wu, C.F. Tsai, K.Y. Yeh, J. Appl. Electrochem. 38 (2008) 507.
[15] G.F. McLean, T. Niet, S. Prince-Richard, N. Djilali, Inter. J. Hydrogen Energy 27 (2002) 507.
[16] T.C. Liu, Y.Y. Li, Carbon 44 (2006) 2045.
[17] H. Arai, S. Müller, O. Hass, J. Electrochem. Soc. 147 (2000) 3584.
[18] G. Wang, Z. Shao, Z. Yu, Nanotechnology 18 (2007) 205705.
[19] O.A. Petrii, J. Solid State Electrochem. 12 (2008) 609.
[20] A.J. Dickinson, L.P.L. Carrette, J.A. Collins, K.A. Friedrich, U. Stimming, J. Appl. Electrochem. 34 (2004) 975.
[21] M.C. Tsai, T.K. Yen, Z.Y. Juang, C.H. Tsai, Carbon 45 (2007) 383.
[22] M.C. Tsai, T.K. Yeh, C.H. Tsai, Electrochem. Commun. 8 (2006) 1445.